Wave-Front Engineering by Huygens-Fresnel Principle for Nonlinear Optical Interactions in Domain Engineered Structures

Yi-qiang Qin, Chao Zhang, Yong-yuan Zhu,* Xiao-peng Hu, and Gang Zhao

National Laboratory of Solid State Microstructures, Nanjing University, Nanjing 210093, China

(Received 7 March 2007; revised manuscript received 18 June 2007; published 12 February 2008)

Wave-front engineering for nonlinear optical interactions was discussed. Using Huygens-Fresnel principle we developed a general theory and technique for domain engineering with conventional quasi-phase-matching (QPM) structures being the special cases. We put forward the concept of local QPM, which suggests that the QPM is fulfilled only locally not globally. Experiments agreed well with the theoretical prediction. The proposed scheme integrates three optical functions: generating, focusing, and beam splitting of second-harmonic wave, thus making the device more compact.

DOI: 10.1103/PhysRevLett.100.063902 PACS numbers: 42.15.Dp, 42.65.−k, 77.80.Dj, 78.66.−w

The ferroelectric domain structure has been widely used for a variety of applications in both linear and nonlinear optics due to its multifunctional properties. In linear optics, it can be used for wave-front controlling by electro-optic effect with lens- or prism-like domain morphology [1,2]. In nonlinear optics, the study of quasi-phase-matching (QPM) has become a hot topic recently [3–9]. QPM can be realized in a ferroelectric crystal by an artificial modulation of its second-order nonlinearity. The structure may be one-dimensional (1D) or two-dimensional (2D), periodic or quasiperiodic [10–17]. Recently, a homocentrically poled $LiNbO_3$ and annular symmetry nonlinear frequency converters have been used to increase the angle acceptance and widen phase mismatch tolerance of second-harmonic generation (SHG) [18,19]. Parametric interactions in transversely patterned QPM gratings (with the periodicity still holding in the longitudinal direction) [20,21] and even disordered domain structures [22] have attracted considerable attention. In Ref. [21], the classical Fraunhofer diffraction and the focusing of SH beam have been demonstrated. Until now, basically, most of parametric interactions realized in different domain engineered structures are totally treated in the framework of conventional QPM configuration. For QPM to be realized, the wave vectors (including the reciprocal vectors) should all be well defined. However, if the wave vectors are not well defined, would it be possible to develop a method with which nonlinear optical parametric interaction can be realized efficiently?

It is well known that Huygens-Fresnel principle (HFP) plays an important role in classical optics. Normally, this process is performed in linear optics regime and in real space. In our present Letter, we extend the HFP to nonlinear optical parametric processes induced by second-order nonlinearity. That is, each point on the primary wave-front acts as a source of secondary wavelets of the fundamental as well as a source of, for example, the SH wave. As an example of proposed method, here the HFP is used to design the domain structure, in which SH output can be controlled and focused into several points. The system acts as a complex lens for SH output; thus, the proposed scheme may be also called wave-front engineering. Both theoretical and experimental results are reported. The concept of local QPM is put forward to explain the observed phenomenon. The proposed scheme can overcome the difficulties confronted either in structures without well-defined reciprocal vector or in optical interacting waves without well-defined wave vectors such as for Gaussian beams.

In order to elucidate the above idea, we consider, as an example, the case of SHG in a domain engineered $LiTaO_3$ crystal. The input fundamental wave is a plane wave propagating along the x direction in the structure, and the generated SH is focused into n points on the focal plane, all z polarized. Usually, the domain pattern can be taken to be uniform in depth (the z direction); the system then simplifies to a 2D system, denoted as xy-plane. Within the plane, the light propagation is isotropic. The multiple reflections, leading to photonic band-gap effects, are not present in this system due to the linear dielectric constant being constant in the whole structure. In such a 2D structure, the problem can be considered as scalar [23], which simplifies the notation. Under the slowly varying envelope approximation [24], the evolution of the second-harmonic amplitude can be written as a function of the pump field and the second-order coefficient $\chi^{(2)}$ [13]:

$$\vec{k}^{2\omega}\cdot\vec{\nabla}[E^{2\omega}(\vec{r})] = -2i(\omega^2/c^2)[E^{\omega}(\vec{r})]^2\chi^{(2)}(\vec{r}) \times \exp\{-i[2\vec{k}^{\omega}(\vec{r}) - \vec{k}^{2\omega}(\vec{r})]\cdot\vec{r}\}. \quad (1)$$

Here, $\vec{r}\equiv(x,y)$ is the 2D spatial coordinate. Generally, $E^{2\omega}$, E^{ω}, $\vec{k}^{2\omega}$, and $\vec{k}^{\omega}$ are all spatial dependent. The nonlinear harmonic components can be described physically by HFP. Because of nonlinearity in the atomic response, each atom develops an oscillating dipole moment which contains a component at frequency 2ω. Here, a small part of crystal containing an enormous number of atomic dipoles can be regarded as a point source which emits SH wave through stimulated dipoles oscillation. The initial phases of these radiations are determined by the phases of the incident fields, and modulated by the 2D domain engineered structure. In the case of focused SHG, the wave vectors $\vec{k}^{2\omega}(\vec{r})$ are spatial-dependent in the crystal. The SH wave focused at point (X_i, Y_i) propagated from the source at (x, y) with sample size $dxdy$ is given:

$$dA_i^{2\omega} = -i\frac{1}{\sqrt{R_i(x,y)}}Kf(x,y)(A^{\omega})^2 \times \exp[-i\Delta\varphi_i(x,y)]dxdy. \quad (2)$$

Here, K is the coupling coefficient, and $f(x, y)$ is a 2D domain structural function. The distance between a point source and focused SHG point is $R_i(x,y) = \sqrt{(X_i - x)^2 + (Y_i - y)^2}$. The factor $1/\sqrt{R_i}$ represents the decay law for amplitude of cylindrical wave and $A_j = \sqrt{n_j/\omega_j}E_j$ $(j = \omega,\ 2\omega)$, respectively. It is noted that $\Delta\varphi_i(x,y) = [2\vec{k}^{\omega}(r) - \vec{k}^{2\omega}(r)]\cdot\vec{r}$, the phase mismatch between the fundamental and harmonic waves, depends on the positions of both the point sources and the focused SHG points. For determination of structural function $f(x, y)$, we derived the following correlation function:

$$F(x,y) = \sum_{i=1,n}\frac{C_i}{\sqrt{R_i}}\exp\{-i[2\vec{k}^{\omega}\cdot\vec{r}(x,y) - \vec{k}^{2\omega}\cdot\vec{r}(x,y)]\} \quad (3)$$

where C_i are the adjustable parameters related to the intensity distribution among focused points; n is the number of multifocused SHG points. Here, the "correlation" means that the change of the coordinates of any one focused point will change the value of $F(x, y)$, even change its sign, and thus change the whole domain structure as can be seen below.

For the input being a plane wave, its phase function reduces to $k^{\omega}x$ and

$$\Delta\varphi_i(x,y) = 2k^{\omega}x + k^{2\omega}R_i - k^{2\omega}(X_i\cos\theta_{1i} + Y_i\cos\theta_{2i}) \quad (i = 1,\ldots,n). \quad (4)$$

Here, k^{ω} is the well defined wave vector of the fundamental; $\cos\theta_{1i}$ and $\cos\theta_{2i}$ are the directional cosines of $k^{2\omega}(\vec{r})$. Here, the correlation function plays the same role as the continuous-valued function [25]. Setting the solutions of $F(x, y) = 0$ to be the locations of the domain wall, the structural function $f(x, y)$ is determined:

$$f(x,y) = \begin{cases} 1, & \mathrm{Re}[F(x,y)] \geq 0 \\ -1, & \mathrm{Re}[F(x,y)] < 0 \end{cases}. \quad (5)$$

By calculating the integral over the whole system, the focused SHG at spatial points can be obtained.

Formulas (1)–(5) constitute the basis of a general theory for domain engineering with conventional QPM structures being the special case. As an example, wave-front engineering for the multifocused SHG by HFP is discussed.

Based on the above theory, the 2D domain structures for the focused SHG are calculated. As a demonstration, Fig. 1 shows the ferroelectric domain structures with the focused points designed to be on the exit surface of the crystal. Obviously, the domain modulation is quite different from the conventional 1D and 2D structures. Figure 1(a) shows the domain structure for the single focused SHG. Near the focused point, the domain boundary curves strongly, whereas far away from the focused point, the domain morphology looks like the conventional 1D periodic structure [as shown in the inset of Fig. 1(a)] which approaches the case investigated in Ref. [21].

Figure 1(b) shows the domain structures for the dual focused SHG. The conventional stripelike domains break into small bricks. The domain structures for the decal focused SHG becomes strange as shown in Fig. 1(c). Because of these domain structures, the SH wave-front generated from a fundamental plane wave is no longer a plane wave-front; rather, it becomes very complicated depending on the number of focused points, resulting in that the conventional QPM is no longer valid.

In order to verify the above scheme, we performed the experiments on focused SHG. The sample was fabricated by poling a 0.5 mm thick z-cut $LiTaO_3$ single domain wafer at room temperature. The domain structure was designed such that the single focused SHG or dual focused SHG for the fundamental 1319 nm z-polarized can be realized with the focused points located 10 cm away from the exit surface. For dual focused SHG, the two focused points are 2 mm apart. In general $f(x, y)$ can

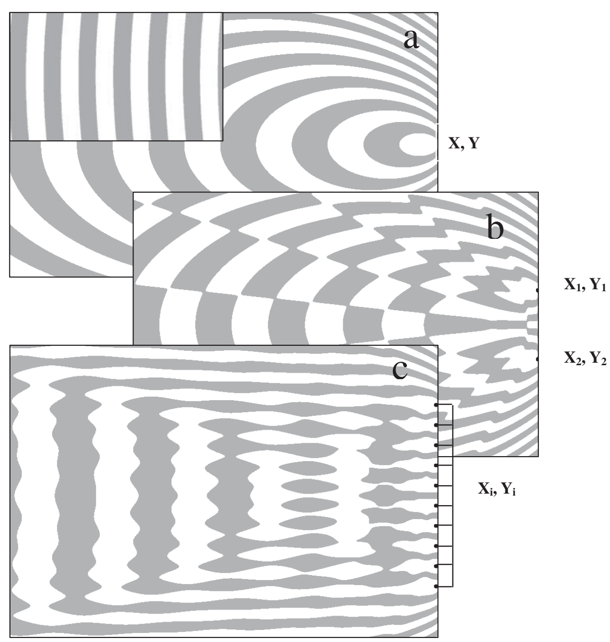

FIG. 1. The schematic diagram of ferroelectric domain structures for (a) single focused SHG (The inset is the domain morphology far from the focal point.), (b) dual focused SHG, and (c) decal focused SHG. The focused points are indicated by (X_i, Y_i).

have a number of domains whose sizes are shorter than the critical size (about 2 μm in our experiment). Because of the electric-poling limits of domain size, in the design, we merge those domains smaller than 2 μm with the adjacent domains. According to our calculation, such technical limits will influence the SH conversion efficiency [10], but keep almost the same focusing features.

SHG of fabricated samples with 10 mm length and 3 mm width was tested using a mode-locked Nd:YAG laser system with a pulse width of 150 ns and a repetition rate of 4 kHz. The fundamental wave was coupled into the polished end face and propagated along the x axis of the sample. Three samples were tested: periodic sample, samples with single focused SHG, and dual focused SHG, whose corresponding domain structures are exhibited in the bottom insets of Fig. 2.

Using a weakly focused fundamental beam by a 15 cm focal-length lens, the waist inside the sample is $\sim$300 μm where the intensity drops to $1/e^2$ of the maximum value and the confocal parameter for the system is $Z_0 \sim 10$ cm much larger than the sample length 10 mm. Thus the fundamental beam can be considered as a plane wave. Figure 2 shows the SHG output CCD images for three different samples. Figure 2(a) exhibits the SHG image in periodic sample, corresponding to the conventional 1D QPM scheme. The beam waist of red SHG is a little bit smaller ($\sim$80%) than the waist of the input fundamental beam. Figures 2(b) and 2(c) show the experimental results of the single and dual focused SHG (The calculated results are shown in the top insets). Figure 2(b) shows the single focal SHG output with its beam waist considerable smaller. Figure 2(c) corresponds to the situation of dual focused SHG. By using bricklike domains with neither translational nor annular symmetry, wave-fronts of SHG are controlled to be convergent towards the two focal points. In both cases, the measured SH minimum waists are about 120 μm, agreeing well with the simulation result.

The SH powers are measured using a Si-calibrated field master detector. In the measurement with the fundamental power 260 mW, the average SH outputs are 110 and 63 mW in 1D periodic and bricklike structures, respectively. Here, 42% SH conversion efficiency is achieved in periodic structure, 24% in bricklike structures. Experimental data also indicate almost the same SHG efficiency is obtained in 1D periodic structure and single focused SHG structure.

For deep understanding of the physical nature of wave-front engineering by HFP, the Fourier spectra of the 2D domain structure for dual focused SHG are studied theoretically and experimentally. A He-Ne laser beam (632.8 nm) is used to scan the z surface of the sample horizontally and vertically. The diffraction pattern is projected onto a screen and recorded by a CCD camera. The Fourier transformation is performed numerically. Figure 3 is the measured (a) and calculated (b) diffraction patterns obtained along the vertical direction. From the results, some distinct features can be revealed. The most noticeable

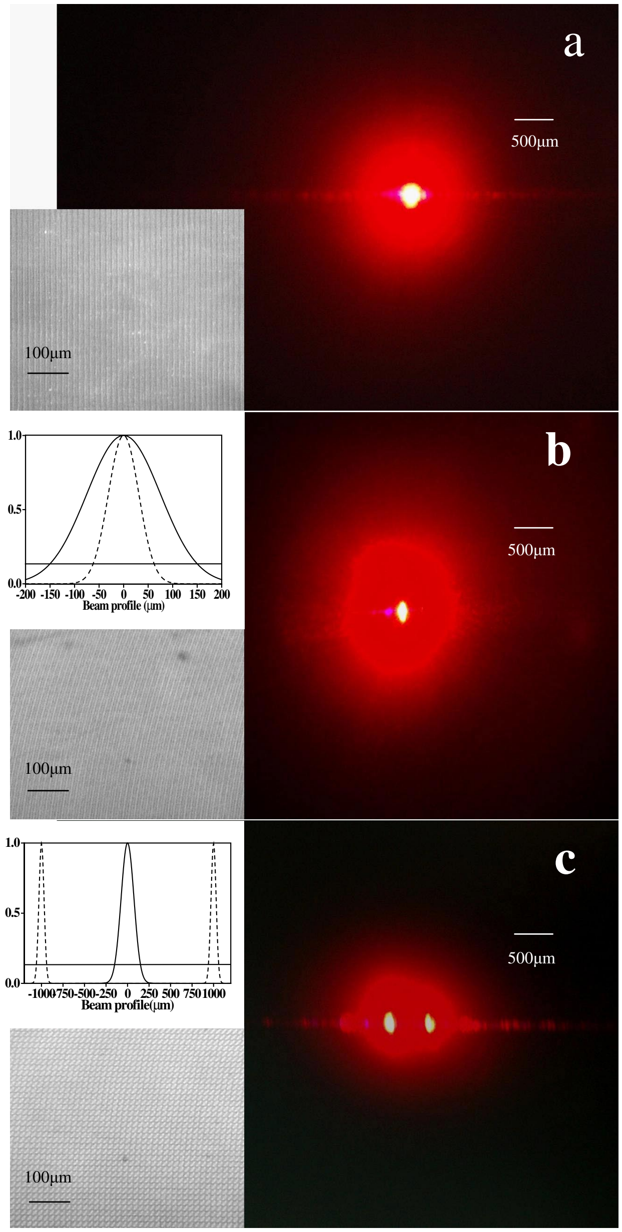

FIG. 2 (color online). CCD images of SHG generated from (a) a periodic domain structure, (b) a domain structure for single focused SHG, and (c) a domain structure for dual focused SHG, respectively. The bottom insets are their corresponding optical microscopic images of domain structures revealed by etching. The top insets in (b) and (c) are the calculated beam profiles of input fundamental wave (solid lines) and output SH wave (dashed lines) at focusing plane.

diffraction spots lay mainly in the second and forth quadrant for the upper patterns and in the first and third quadrant for the bottom patterns. They show mirror symmetry with each other, which reflects the symmetry of domain pattern in real space. The symmetries of these patterns are totally different from the symmetry of the middle ones. This indicates the reciprocal vectors are spatial dependent. Actually, in the experiments, when moving the laser

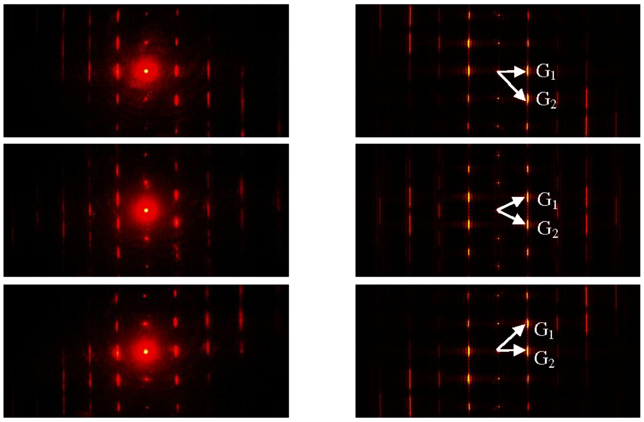

(a) (b)

FIG. 3 (color online). Fourier spectra of domain structure shown in the inset of Fig. 2(c) for dual focused SHG obtained along the vertical direction: (a) the experimental and (b) the calculated results. The schematic diagrams of local QPM are indicated.

beam vertically from the upper part to the bottom part, the diffraction pattern has been observed to change gradually. The diffraction pattern changes slightly along the horizontal direction due to the fact that the focused points are designed rather far from the exit face of the sample. From the diffraction pattern exhibited above, it seems possible to define the so-called local QPM condition although the QPM condition could not be fulfilled globally. That is, the phase mismatch can be compensated locally with reciprocal vectors provided by local structure. In Fig. 3(b), we schematically show the reciprocal vectors used for local QPM, where G_1 is used for the upper focal point and G_2 for the lower one.

It is interesting to compare the conventional QPM structure to current domain structure. When the single focused point of SHG is designed to be located infinitely, 2D modulated structure function $f(x, y)$ degenerate into that of conventional 1D QPM structure with the period of $2\pi/(k^{2\omega} - 2k^{\omega})$. The structure can also degenerate into the conventional 1D structure when the focused points on the focal plane approach infinity. Moreover, when multi-focused points of SHG are located infinitely at two perpendicular directions, the structure becomes the 2D periodic structure.

The advantage of the proposed scheme lies in its capability to perform several functions with a special designed domain structure. As one of the perspectives for application, the example presented above combines three functions: SHG, focusing, and beam splitting, thus making the device more compact. The method can also be used for the tight focused Gaussian beam with which the efficient frequency conversion does not occur at phase-matching condition [24,26] and extended to other parametric processes such as down conversion. Studies on these processes by using local QPM are of potential interest in photonic applications. Thus, HFP may play an important role in nonlinear optical field with engineered domain structures.

This work was supported by the State Key Program for Basic Research of China (Grants No. 2004CB619003 and No. 2006CB921804) and the National Natural Science Foundation of China (Grants Nos. 10523001, 10504013, and 10674065).

*Corresponding author

[1] Y. Chiu, D. D. Stancil, and T. E. Schlesinger, Appl. Phys. Lett. **69**, 3134 (1996).
[2] M. Yamada, M. Saitoh, and H. Ooki, Appl. Phys. Lett. **69**, 3659 (1996).
[3] G. D. Miller R. G. Batchko, W. M. Tulloch, M. M. Fejer, and R. L. Byer, Opt. Lett. **22**, 1834 (1997).
[4] M. A. Arbore A. Galvanauskas, D. Harter, M. H.Chou, and M. M. Fejer, , Opt. Lett. **22**, 1341 (1997).
[5] S. N. Zhu *et al.*, Phys. Rev. Lett. **78**, 2752 (1997); L. Noirie, P. Vidakovic, and J. A. Levenson, J. Opt. Soc. Am. B **14**, 1 (1997); P. Unsbo, *ibid.* **12**, 43 (1995); G. I. Stegeman M. Bahae, E. W. Van Stryland, and G. Assanto, Opt. Lett. **18**, 13 (1993).
[6] M. Tiihonen, V. Pasiskevicius, and F. Laurell, Opt. Express **12**, 5526 (2004).
[7] L. Torner, C. R. Menyuk, and G. I. Stegeman, Opt. Lett. **19**, 1615 (1994).
[8] A. Stabinis, G. Valiulis, and E. A. Ibragimov, Opt. Commun. **86**, 301 (1991).
[9] G. Assanto *et al.*, Appl. Phys. Lett. **67**, 2120 (1995).
[10] M. M. Fejer *et al.*, IEEE J. Quantum Electron. **28**, 2631 (1992).
[11] Y. Y. Zhu and N. B. Ming, Quantum Electron. **31**, 1093 (1999).
[12] K. Fradkin-Kashi, A. Arie, and G. Rosenman, Phys. Rev. Lett. **88**, 023903 (2001).
[13] V. Berger, Phys. Rev. Lett. **81**, 4136 (1998).
[14] N. G. Broderick *et al.*, Phys. Rev. Lett. **84**, 4345 (2000).
[15] L. H. Peng *et al.*, Appl. Phys. Lett. **84**, 3250 (2004).
[16] B. Q. Ma *et al.*, Appl. Phys. Lett. **87**, 251103 (2005).
[17] R. Lifshitz, A. Arie, and A. Bahabad, Phys. Rev. Lett. **95**, 133901 (2005).
[18] T. Wang *et al.*, Opt. Commun. **252**, 397 (2005).
[19] D. Kasimov *et al.*, Opt. Express, **14**, 9371 (2006).
[20] G. Imeshev, M. Proctor, and M. M. Fejer, Opt. Lett. **23**, 673 (1998).
[21] J. R. Kurz *et al.*, IEEE J. Sel. Top. Quantum Electron. **8**, 660 (2002).
[22] M. Baudrier-Raybaut *et al.*, Nature (London) **432**, 374 (2004).
[23] P. R. Villeneuve and M. Piche, Phys. Rev. B **46**, 4969 (1992).
[24] R. W. Boyd, *Nonlinear Optics* (Academic Press, New York, 2003).
[25] T. Kartaloglu, Z. G. Figen, and O. Aytur, J. Opt. Soc. Am. B **20**, 343 (2003).
[26] G. D. Xu *et al.*, J. Opt. Soc. Am. B **20**, 360 (2003).